Research Article Vol. 29, No. 2 / 18 January 2021 / Optics Express 2387
Optics EXPRESS

Room temperature, nanosecond, 60 mJ/pulse Fe:ZnSe master oscillator power amplifier system operating at 3.8-5.0 µm

DMITRY MARTYSHKIN,* KRISHNA KARKI, VLADIMIR FEDOROV, AND SERGEY MIROV

Department of Physics, University of Alabama at Birmingham, CH 310, 1300 University Blvd., Birmingham, AL 35294, USA
dmartych@uab.edu

Abstract: We report on a RT gain-switched Fe:ZnSe master oscillator power amplifier (MOPA) system tunable over 3.8–5.0 µm pumped by radiation of Er:YAG laser operating at 2.94 µm. The mechanically Q-switched Er:YAG laser with output energy up to 220 mJ was used as a pump source for a master oscillator and three-stage power amplifier. The maximum output energies in 200 ns pulses exceeded 60, 56, and 48 mJ at 4.4, 4.3, and 4.1 µm, respectively, under 220 mJ of pump energy. The extraction energy efficiencies were measured to be 25, 30, and 40% at the first, second, and third stages, respectively.

1. Introduction

A variety of scientific, industrial, and medical applications require high energy, tunable middle-infrared (mid-IR) solid state laser systems operating at room temperature (RT). Laser oscillation in mid-IR wavelengths can be achieved by several techniques including nonlinear frequency conversion, lead-salt diode lasers, antimonide lasers, quantum cascade lasers, and rare-earth doped, as well as transition metal (TM) doped crystalline lasers. Among other solid-state lasers, mid-IR lasers based on transitions of TM^{2+} ions in tetrahedral crystalline sites demonstrate impressive output characteristics. TM^{2+} doped wide bandgap II-VI semiconductor crystals were first introduced to the scientific community as effective mid-IR gain media by scientists from the Lawrence Livermore National Laboratory (LLNL) [1,2]. II-VI chalcogenides crystallize as tetrahedrally coordinated structures enabling small crystal field splitting of the TM ions in comparison with typical octahedral coordination sites, placing TM ion transitions in the mid-IR spectral range. The heavy anions of II-VI chalcogenides enable a low energy optical phonon cut-off for these crystals. This makes them transparent over a wide spectral range, decreases the efficiency of impurity non-radiative decay, and makes them promising hosts for effective mid-IR lasing at RT and above. Among the TM ions, ^5D ions (such as $Cr^{2+}$and Fe^{2+}) are the most attractive for laser applications. The ^5D ground state of these ions is split into $^5T_2$ triplet and ^5E duplet in the tetrahedral crystal field of II-VI chalcogenides. The transitions between these levels are in the mid-IR spectral range and feature broad absorption and emission bands as well as high ($\sim 10^{-18}$ cm^2) cross-sections. All the transitions to other multiplets are spin forbidden. Crystal field splitting of the Fe^{2+} ions is smaller in comparison with Cr^{2+} ions, therefore iron-doped chalcogenides are well recognized materials of choice for direct lasing over the 3–7 µm spectral range [3–7]. While variations of chalcogenide host compounds allows one to extend the tunability range to more than one octave, the best output laser characteristics were demonstrated using Fe:ZnSe gain elements. Figure 1(i) shows mid-IR transmission of the Fe:ZnSe crystals used in further experiments as well as the emission cross-section at the $^5T_2 \rightarrow {}^5E$ transition of the Fe^{2+} ions.

#416574 https://doi.org/10.1364/OE.416574
Journal © 2021 Received 3 Dec 2020; revised 22 Dec 2020; accepted 23 Dec 2020; published 13 Jan 2021

Optics EXPRESS

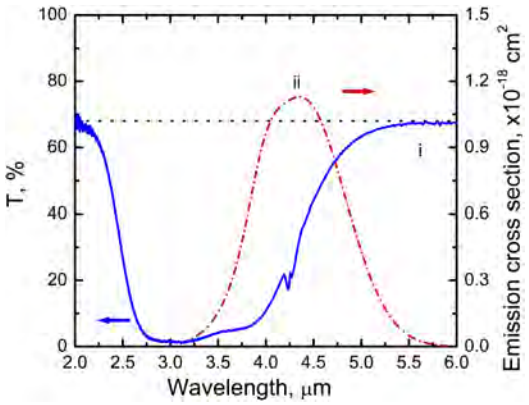

Fig. 1. Transmission spectrum of uncoated 1.8 mm long Fe:ZnSe gain element (i, solid blue line) identical to the AR coated elements used in MOPA; RT emission cross-section spectrum of Fe^{2+} ions (ii, dash-dot red-line); dotted line shows calculated Fresnel transmission of the ZnSe.

This $^5E \leftrightarrow {}^5T_2$ transition of the Fe^{2+} ions in ZnSe features a combination of high peak absorption (1.1×10^{-18} cm^2) and emission (1.3×10^{-18} cm^2) cross-sections with broad absorption (2.5–4.5 μm) and emission (3.5–5.2 μm) bands [4,6]. The lifetime of the upper laser level $^5T_2$ of the Fe^{2+} ion in ZnSe crystals falls with temperature from τ=57 μs at 120 K to 370 ns at RT due to the increase of nonradiative relaxation [8]. These lifetimes enable effective laser oscillation under 2.94 μm Er:YAG laser pumping in free running and gain-switch regimes at low and RT, respectively. After the first RT Fe:ZnSe lasing was demonstrated in [9], high output energy RT gain-switched oscillations of the Fe:ZnSe laser were reported by several research groups [10,11] with a maximum output energy of ~1.4 J at 150 ns pulse duration demonstrated when pumped by the radiation of a Hydrogen-Fluoride (HF) laser [12]. However, the usage of a toxic HF gas laser limits the number of possible applications. In our paper, we report on the development of a tunable 3.8–5.0 μm Fe:ZnSe solid-state MOPA system operating at RT pumped by the radiation of a mechanically Q-switched Er:YAG laser. The design of a high energy Fe:ZnSe system can be based either on a high energy master oscillator or more complex MOPA architectures. Since our objective was to develop a narrow-line (<1 nm) broadly tunable system requiring the use of a low optical damage, highly dispersive diffraction grating, we have chosen the MOPA approach.

2. Experimental setup

The optical scheme of a tunable Fe:ZnSe MOPA system is shown in Fig. 2. Fe^{2+} doped ZnSe polycrystals were used as gain elements in the MOPA system. The iron concentration and crystal thickness were optimized to achieve an initial absorption at pump wavelength of ~ 98% at crystal lengths of 2–3 mm and Fe concentrations of ~ 1.5×10^{19} cm^{-3}. Doping was accomplished in vacuum-sealed ampoules using post-growth thermal diffusion of iron from Fe metal films deposited on crystals that were grown utilizing a chemical vapor transport technique. The gain elements have anti-reflection coatings with residual reflection coefficients less than 1% at the pump wavelength and over the 3.9–5.0 μm spectral range.

A home-made mechanically Q-switched Er:YAG laser operating at 2.94 μm and a 3 Hz repetition rate was used as a pump source for the RT Fe:ZnSe MOPA system. The laser cavity was formed by a flat back mirror and a flat output coupler with a reflectivity of 75%. The mechanical Q-switching was realized via spinning of the flat back mirror. Laser stability was provided by a thermal lens in the Er:YAG crystal. In our experiments, we used a 120 mm long Er (50%):YAG crystal with a 7 mm diameter. The rod had AR-coatings on both end surfaces. The maximum

Optics EXPRESS

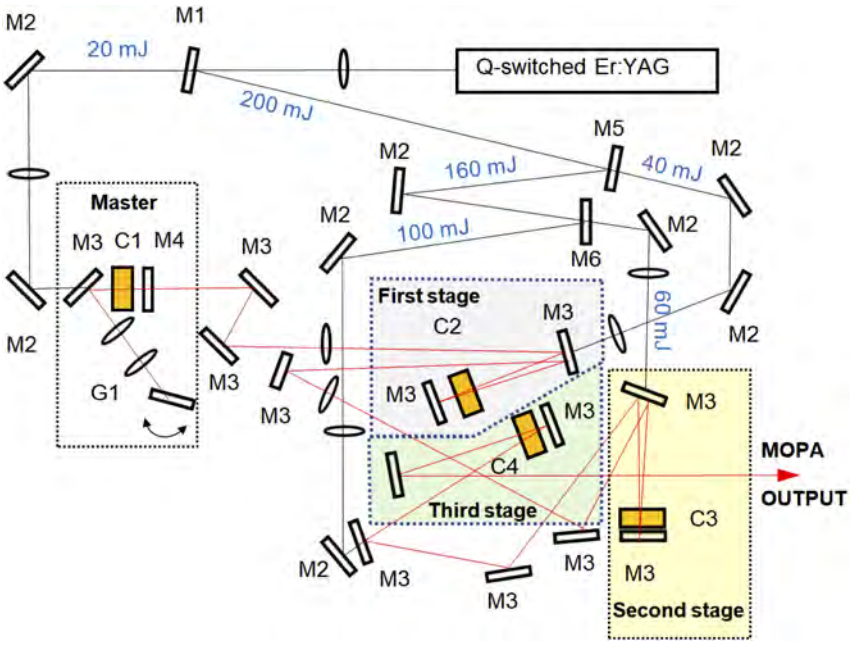

Fig. 2. Optical scheme of the Fe:ZnSe master oscillator and 3 stage power amplifier: M1 – Partial reflector at 2.94 μm, R=90%, M2 - High reflector at 2.94 μm, M3 – High Reflector at 3.5–5.3 μm, high transmission at 2.9 μm, M4 - Partial reflector at 3.5–5.3 μm, R=70%, M5 - Partial reflector at 2.94 μm, R=80%, M6 - Partial reflector at 2.94 μm, R=60%, G1 - Diffraction grating 300 g/mm, C1 - C4 - Fe:ZnSe gain elements.

output energy of the Q-switched Er:YAG laser used in our experiments was as high as 250 mJ in ~ 200 ns pulses. However, in our experiments, we used ~220 mJ of the total pump energy due to the losses on beam steering mirrors and uncoated lenses. The output beam of the pump laser was split by partial reflectors M1, M5, and M6 on the 20, 40, 60, and 100 mJ beams, which were used for the pumping of the master oscillator, 1st, 2nd, and 3rd cascades of the power amplifier, respectively. Dichroic mirrors M2 with a high reflectivity at pump wavelength were used for steering of the pump radiation. Mirrors M3 have a high reflectivity (R > 99%) over the 3.5–5.3 μm spectral range and a high transmittance (T > 95%) at the pump wavelength and were used for steering laser radiation and separation of the residual pump from the Fe:ZnSe laser radiations.

The RT gain-switched Fe:ZnSe master oscillator tunable over 3.60–5.15 μm and pumped by 2.94 μm radiation was reported earlier [13]. We used a folded cavity design to avoid incidence of the pump radiation on the diffraction grating G1 and to decrease the energy density on the folded mirror. To obtain a narrow-line tunable oscillation, the back mirror was replaced by the diffraction grating G1 (300 gr/mm) with a diffraction efficiency >80% operating in the Littrow mount auto-collimation regime. An intracavity telescope based on AR coated CaF_2 lenses was installed into the cavity to reduce the energy density on the diffraction grating and to increase the grating resolving power. The output coupler has ~50% reflectivity over the Fe:ZnSe tuning range. The pump-focusing lens and steering mirror were used to control the pump area on the surface of the gain element. The maximum output energy in the dispersive cavity was measured to be 4 mJ. However, after the beam steering and the use of uncoated optical elements only ~ 2.3 mJ at 4.4 μm and ~ 1.5 mJ at 4.1 μm were delivered to the first gain element. The tuning range spans over the 3.60–5.15 μm spectral range.

Optics EXPRESS

A quasi-collinear configuration with a double-pass propagation of the seed beam was utilized in the 3-stage amplifier. The pump and seed beams were focused by lenses to beam diameters enabling a pump energy density of ~ 1 J/cm^2 at the maximum pump energy for each cascade.

3. Experimental results and discussion

Output energies at 4.1 μm and 4.4 μm depicted after first, second, and third amplification stages are shown in Fig. 3. The output energy extracted from each amplification stage linearly increased with increasing pump energy. The difference between the output energy of the previous cascade and the input energy of the following cascade was due to suboptimal reflection of the steering mirrors M3 positioned at different incident angles, the usage of uncoated focusing lenses, and losses due to residual absorption in the insufficiently pumped Fe:ZnSe gain element of the next amplifier stage. We achieved output energies of 12 (8), 31 (22) and 60 (48) mJ at 4.4 (4.1) μm in the 1st, 2nd and 3rd stages of the amplifier, respectively, with a total amplifier pump energy of 200 mJ. There was no roll-off from the linear dependence at each of the amplification stages. The extraction energy efficiencies [(E_{out}-E_{in})/E_{pump}] at 4.4 μm were measured to be 25%, 30%, and 40% at the first, second, and third stages, respectively. The total efficiencies of the amplifier at the maximum pump energy were measured to be 28% and 23% at 4.4 and 4.1 μm, respectively. We observed no amplified spontaneous emission and no optical damage of the Fe:ZnSe gain elements throughout the experiments.

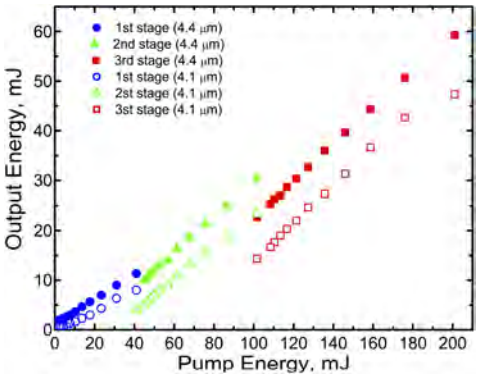

Fig. 3. Output energy extracted from the three-stage Fe:ZnSe power amplifier at 4.4 μm (solid symbols) and 4.1 μm (open symbols) wavelengths.

The temporal profile of the typical pump and pulses at 4.4 μm are shown in Fig. 4(A). The seed pulse consists of a sharp spike followed by a longer ~ 200 ns tail. The amplification of the seed pulses resulted in some saturation of the initial spike while maintaining approximately the same pulse duration. Figure 4(B) depicts the spectral outputs of the seed laser operating at ~ 4.1 μm and the MOPA system after the 3rd amplification stage. As one can see from Fig. 4(B), the linewidth of the seed laser was measured to be 1.0 nm at full width half maxima (FWHM) and was slightly increased to ~ 2.0 nm after the third amplification stage.

The spatial beam profiles, as depicted in Fig. 5, are rather smooth without any hot spots. It should be noted that there were only minor beam distortions in the amplification cascades in comparison with the seed beam. The output beam after the third cascade was slightly astigmatic with an estimated divergence of ~ 8 mrad. We believe that the spatial profiles of the MOPA output beam could be further improved by improving the seed beam quality.

We did not observe any influence of amplified spontaneous emission on the output parameters over the 4.1–4.4 μm tuning range. However, as shown in Fig. 6(A), in the absence of the seed pulse, we observed nonselective two pass amplification due to a coupling of the multi-stage

Optics EXPRESS

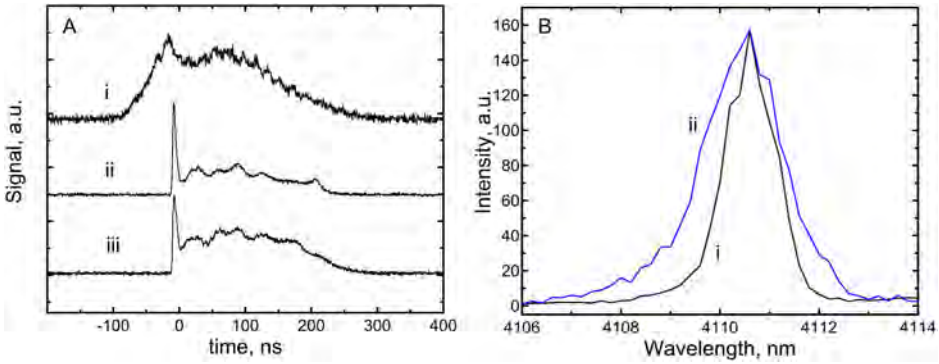

Fig. 4. (A) Typical temporal profiles of the pump at 2.94 μm and Fe:ZnSe pulses at 4.4 μm: A(i) Er:YAG pulse duration at 2.94 μm; A(ii) pulse duration of master oscillator; A(iii) pulse duration at 3rd amplification stage. (B) Spectral Profiles of Fe:ZnSe System: B(i) output spectrum of master oscillator at 4.1 μm; B(ii) output spectrum at the 3rd amplification stage.

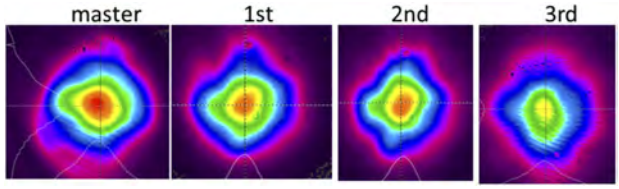

Fig. 5. Seed and output beam profiles of the multi-stage Fe:ZnSe power amplifier, after the first, second and third stages, respectively.

amplifier with the output coupler of the master oscillator. The blue curve demonstrates the spectrum of the amplified radiation at 4.1 μm, while the red curve shows the output radiation without seed pulses. As one can see, there is non-selective broadband parasitic lasing centered at 4.15 μm without the use of seed radiation. Also, parasitic oscillation between 4.0–4.2 μm was detected when the master oscillator wavelength was longer than 4.4 μm. Figure 6(B) shows the output spectra of the MOPA system when the master oscillator wavelength was set at 4.6 μm. One of the simple ways to extend tunability to longer wavelengths without parasitic radiation is to place a 4.0–4.2 μm absorber which can prevent coupling between the master oscillator (MO) and the power amplifier (PA) in this spectral range. An unpumped Fe:ZnSe gain element could be used for this application. As one can see from Fig. 1, due to a strong overlap between Fe:ZnSe absorption and emission bands around 4.0 μm, the gain element provides ~84% absorption in this spectral range while the absorption in the spectral range between 4.6 μm and 5.0 μm varies from 26% to 7%. Figure 6(C) shows the output MOPA spectrum with an unpumped Fe:ZnSe crystal installed between MO and PA. As one can see, placing Fe:ZnSe between MO and PA results in total suppression of parasitic oscillation around 4.15 μm. The suppression of the parasitic oscillation for operation below 4.1 μm could also be achieved by decreasing the pump energy of the first amplification stage. It should be also noted that due to atmospheric CO_2 absorption, we purged the system with argon to suppress a strong intracavity 4.2–4.35 μm absorption to enable effective operation around 4.3 μm. The output characteristics of the purged Fe:ZnSe system at 4.3 μm were very similar to the output characteristics at 4.4 μm without purging with a maximum output energy exceeding 56 mJ under 200 mJ of total pump energy of the 3-stage MOPA.

Figure 7 demonstrates tuning curves of the Fe:ZnSe MOPA under different experimental conditions. The best results were obtained over the 4.1–4.4 μm spectral range as shown in Fig.

Optics EXPRESS

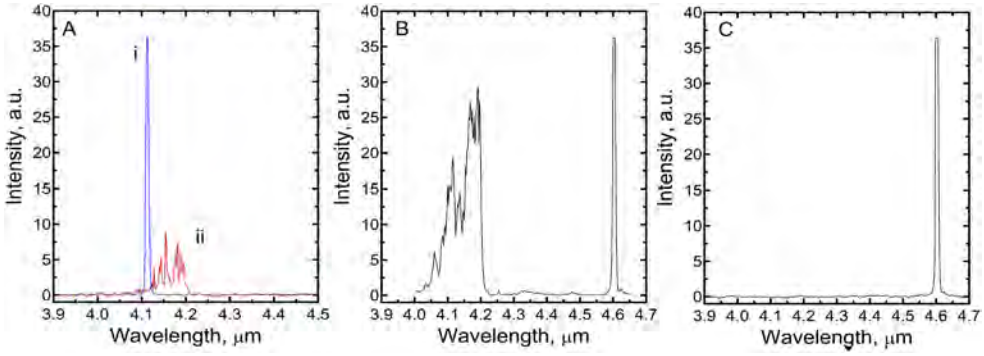

Fig. 6. Emission spectra of the Fe:ZnSe MOPA system: A.(i) at 4.1 μm without absorbing element between MO and PA; A(ii) nonselective two pass amplification due to coupling of the multi-stage amplifier with the master oscillator output coupler; (B) at 4.6 μm without absorbing element between MO and PA; (C) at 4.6 μm with absorbing element between MO and PA.

7(ii). These data were obtained under argon purging without decreased pump energy at the 1st cascade and without an absorbing element between MO and PA. We have not observed any parasitic oscillations over the 4.1–4.4 μm spectral range, however at 4.6 μm and 4.7 μm we observed ~10 mJ of amplified spontaneous emission. Figure 7(iii) shows the tuning curve of the laser system with an absorbing element between MO and PA under ambient atmosphere, while Fig. 7(iv) shows the tuning curve with decreased pump energy of the 1st cascade down to 10 mJ without an absorbing element between MO and PA under ambient atmosphere. Figure 7(i) shows for comparison the master oscillator tuning curve.

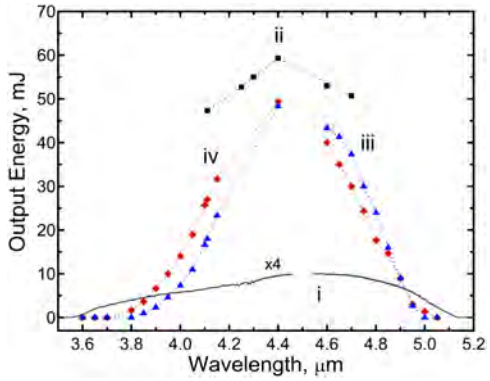

Fig. 7. Tuning curves of Fe:ZnSe MOPA system under different conditions: (i) tuning curve of the master oscillator; (ii) tuning curve at full pump energy without absorbing element between MO and PA; (iii) tuning curve with absorbing element between MO and PA; (iv) tuning curve with decreased pump energy of the 1st cascade down to 10 mJ without absorbing element between MO and PA.

4. Conclusions

In summary, we report on RT gain-switched Fe:ZnSe MOPA systems tunable over 3.8–5.0 μm pumped by 2.94 μm radiation of Er:YAG laser with an approximately 30-fold total gain. A mechanically Q-switched Er:YAG laser with output energy up to 220 mJ was used as a pump

Optics EXPRESS

source for a master oscillator and power amplifier. The maximum output energies in 200 ns pulses exceeded 60, 56, and 48 mJ at 4.4, 4.3, and 4.1 μm, respectively, under 220 mJ of total pump energy. The extraction energy efficiencies were measured to be 25, 30, and 40% at the first, second, and third stages, respectively. The spectral linewidth of the seed laser was slightly increased from 1 nm to 2.0 nm after the third amplification stage.

We observed the influence of parasitic oscillation on the MOPA output characteristics when the master oscillator was tuned to wavelengths longer than 4.6 μm. The influence of parasitic oscillation on the efficiency of RT Fe:ZnSe lasers was also reported in [12]. The suppression of these parasitic processes requires a special design of the gain elements as well as utilization of optical isolators. In our future work, we plan to capitalize on the recently demonstrated mechanically Q-switched Er:YAG laser with an output energy in excess of 800 mJ [14] to energy scale the Fe:ZnSe MOPA system up to ~ 250 mJ.

Funding. Air Force Office of Scientific Research (FA9550-13-1-0234); U.S. Department of Energy (DE-SC0018378); National Institute of Environmental Health Sciences(P42ES027723).

Disclosures. The work reported here partially involves intellectual property developed at the University of Alabama at Birmingham. This intellectual property has been licensed to the IPG Photonics Corporation. Drs. Fedorov, Martyshkin and Mirov declare competing financial interests.

References

1. L. D. DeLoach, R. H. Page, G. D. Wilke, S. A. Payne, and W. F. Krupke, "Transition metal-doped zinc chalcogenides: spectroscopy and laser demonstration of a new of gain media," IEEE J. Quantum Electron. **32**(6), 885–895 (1996).
2. R. H. Page, K. I. Shaffers, L. D. DeLoach, G. D. Wilke, F. D. Patel, J. B. Tassano, S. A. Payne, W. F. Krupke, K. T. Chen, and A. Burger, "Cr^{2+}-doped zinc chalcogenides as efficient, widely tunable mid-infrared lasers," IEEE J. Quantum Electron. **33**(4), 609–619 (1997).
3. S. B. Mirov, V. V. Fedorov, I. S. Moskalev, D. Martyshkin, and C. Kim, "Progress in Cr^{2+} and Fe^{2+} Doped Mid-IR Laser Materials," Laser & Photon. Rev. **4**(1), 21–41 (2010).
4. S. Mirov, V. Fedorov, D. Martyshkin, I. Moskalev, M. Mirov, and S. Vasilyev, "Progress in Mid-IR Lasers Based on Cr and Fe Doped II-VI Chalcogenides," IEEE J. Sel. Top. Quantum Electron. **21**(1), 292–310 (2015).
5. A. D. Martinez, D. V. Martyshkin, R. P. Camata, V. V. Fedorov, and S. B. Mirov, "Crystal field engineering of transition metal doped II-VI ternary and quaternary semiconductors for mid-IR tunable laser applications," Opt. Mater. Express **5**(9), 2036–2046 (2015).
6. S. Mirov, I. Moskalev, S. Vasilyev, V. Smolski, V. Fedorov, D. Martyshkin, J. Peppers, M. Mirov, A. Dergachev, and V. Gapontsev, "Frontiers of mid-IR lasers based on transition metal doped chalcogenides," IEEE J. Sel. Top. Quantum Electron. **24**(5), 1–29 (2018).
7. M. P. Frolov, Y. V. Korostelin, V. I. Kozlovsky, S. O. Leonov, and Y. K. Skasyrsky, "Tunable in the range of 4.5–6.8 μm room temperature single-crystal Fe:CdTe laser pumped by Fe:ZnSe laser," Opt. Express **28**(12), 17449–17456 (2020).
8. N. Myoung, V. V. Fedorov, S. B. Mirov, and L. E. Wenger, "Temperature and concentration quenching of mid-IR photoluminescence in iron doped ZnSe and ZnS laser crystals," J," Luminescence **132**(3), 600–606 (2012).
9. J. Kernal, V. V. Fedorov, A. Gallian, S. B. Mirov, and V. V. Badikov, ""3.9–4.8 μm gain-switched lasing of Fe:ZnSe at room temperature"," Opt. Express **13**(26), 10608–10615 (2005).
10. V. A. Akimov, A. A. Voronov, V. I. Kozlovskii, Y. V. Korostelin, A. I. Landman, Y. P. Podmar'kov, and M. P. Frolov, "Efficient lasing in a Fe^{2+}:ZnSe crystal at room temperature," Quantum Electron. **36**(4), 299–301 (2006).
11. V. V. Fedorov, S. B. Mirov, A. Gallian, D. V. Badikov, M. P. Frolov, Y. V. Korostelin, V. I. Kozlovsky, A. I. Landman, Y. P. Podmar'kov, V. A. Akimov, and A. A. Voronov, "3.77–5.05-mm Tunable Solid-State Lasers Based on Fe^{2+}-Doped ZnSe Crystals Operating at Low and Room Temperatures," IEEE J. Quantum Electron. **42**(9), 907–917 (2006).
12. A. E. Dormidonov, K. N. Firsov, E. M. Gavrishchuk, V. B. Ikonnikov, S. Y. Kazantsev, I. G. Kononov, T. V. Kotereva, D. V. Savin, and N. A. Timofeeva, "High-efficiency room-temperature ZnSe:Fe^{2+} laser with a high pulsed radiation energy," Appl. Phys. B **122**(8), 211 (2016).
13. V. Fedorov, D. Martyshkin, K. Karki, and S. Mirov, "Q-switched and gain-switched Fe:ZnSe lasers tunable over 3.60–5.15 μm," Opt. Express **27**(10), 13934–13941 (2019).
14. K. Karki, V. Fedorov, D. Martyshkin, and S. Mirov, "High Energy Mechanically Q-switched 2.94 μm Er:YAG Laser," *Laser Congress 2020 (ASSL, LAC)* OSA Technical Digest (Optical Society of America, 2020), paper AW4A.6.